Dyes and Pigments 96 (2013) 333–337

Contents lists available at SciVerse ScienceDirect

Dyes and Pigments

journal homepage: www.elsevier.com/locate/dyepig

A fluorescent and colorimetric chemosensor for nitric oxide based on 1,8-naphthalimide

Min Wang [a,b], Zhaochao Xu [b,*], Xu Wang [a,b], Jingnan Cui [a,**]

[a] State Key Laboratory of Fine Chemicals, Dalian University of Technology, Dalian 116024, China
[b] Dalian Institute of Chemical Physics, Chinese Academy of Sciences, Dalian 116023, China

ARTICLE INFO

Article history:
Received 13 July 2012
Received in revised form
22 August 2012
Accepted 23 August 2012
Available online 10 September 2012

Keywords:
Fluorescent chemosensor
Nitric oxide
1,8-Naphthalimide
o-phenylenediamine
Colorimetric
Bioimaging

ABSTRACT

A fluorescent chemosensor N-*n*-butyl-3,4-diamino-1,8-naphthalimide (**DAN**) for detecting NO was developed on the basis of 1,8-naphthalimide with a similar structure of *o*-phenylenediamine as a NO reaction site. Due to the interaction between the photoinduced electron transfer (PET) and the intramolecular charge transfer (ICT), the chemosensor exhibits a remarkable enhancement in the emission intensity that is ca. 160-fold increase and a blue shift in the emission wavelength after the addition of NO. Meanwhile, it displays a colorimetric response accompanied with a color change from yellow to colorless. The chemosensor **DAN** shows a high selectivity for NO in the presence of various reactive nitrogen species (RNS) and reactive oxygen species (ROS). Furthermore, **DAN** can be used for bioimaging of NO in living cells.

1. Introduction

Nitric oxide (NO) is a gaseous radical species with a half-life of a few seconds [1]. It is a ubiquitous signal molecule which plays a critical role in a wide range of physiological activities including endothelial-derived relaxant factor (EDRF) in blood vessels [2], neurotransmitter in the central nervous system [3] and mediator in the immune system [4]. NO is also involved in various pathophysiological processes as a cytotoxic agent. Mis-regulation of NO leads to a number of human diseases like cardiac disorders, gastrointestinal distress and neurodegeneration [5].

Owing to the biological significance of NO in human health and diseases, several methods for the detection of NO have been developed [6,7], among which optical detections have shown a good prospect. Colorimetric detection could simplify the operation and minimize the costs of the instrumentation. Especially, fluorescence has been proved to be an important detection method owing to high sensitivity and, importantly, successful application in biological imaging [8]. Until now, a great number of fluorescent chemosensors for monitoring NO have been developed which can be cataloged into two main types. One type is based on the reaction of *o*-phenylenediamine with NO through the principle of photoinduced electron transfer (PET) [9]. Another one is using transition metal complexes as NO receptors [10]. In our previous studies, various ligands were conjugated to 1,8-naphthalimide which is characteristic of an intramolecular charge transfer (ICT) chromophore with desirable photophysical properties such as a large Stokes' shift and long emission wavelength [11,12] to form a number of colorimetric and ratiometric fluorescent chemosensors for transition metal ions such as Cu(II) [13,14], Zn(II) [15], Cd(II) [16] and Ag(I) [17].

In this paper, our strategy is to introduce a similar receptor site of *o*-phenylenediamine conjugated to 1,8-naphthalimide to make a NO chemosensor. The fluorescent chemosensor for NO, N-*n*-butyl-3,4-diamino-1,8-naphthalimide termed **DAN**, could be easily obtained in a satisfactory yield through simple synthesis. In our work, two amino groups are directly tethered to naphthalimide fluorophore possessing a *push–pull* character to generate a similar structure of *o*-phenylenediamine acting as a NO recognition moiety. Upon selective reaction of **DAN** with NO to produce a triazole ring (Scheme 1), the generation of the triazolate form of **DAN-T** under physiological conditions inhibits the PET effect of 3-amino together with the ICT of 4-amino in 1,8-naphthalimide to induce the changes of fluorescence and absorption spectra.

* Corresponding author.
** Corresponding author.
E-mail addresses: zcxu@dicp.ac.cn (Z. Xu), jncui@dlut.edu.cn (J. Cui).

0143-7208/$ – see front matter © 2012 Elsevier Ltd. All rights reserved.
http://dx.doi.org/10.1016/j.dyepig.2012.08.024

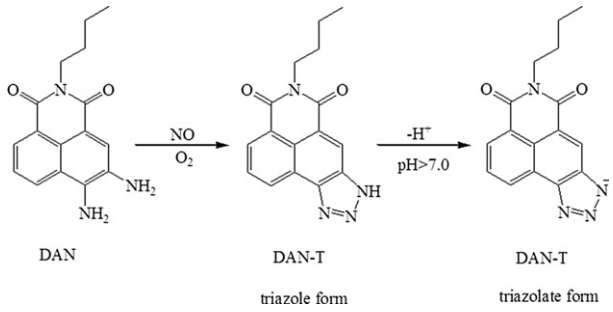

Scheme 1. The reaction process of **DAN** with NO.

2. Experimental

2.1. Materials and instruments

Unless otherwise noted, all reagents were commercial and used without further purification. Deionized water was used throughout all experiments. Silica gel (100–200 mesh) was used for column chromatography. Mass determination was made on a GC-TOF MS spectrometry. NMR spectra were recorded on a Varian 400 MHz with chemical shifts reported as ppm (in DMSO-d_6, TMS as internal standard). Fluorescence measurements were performed on a FP-6500 spectrophotometer (Jasco, Japan) and the slit width were 5 nm and 2.5 nm for excitation and emission, respectively. Absorption spectra were measured on a Lamda LS35 spectrophotometer.

NO, ClO^- were produced from the dissolution of NOC13 (a white solid acting as NO source, 13.7 min of the half-life) [18] and NaOC1 in the water, respectively. H_2O_2 was diluted from a stabilized 30% H_2O_2 solution. The equivalent of NaOC1 and H_2O_2 was to generate $^1O_2$. •OH was prepared from the reaction of the equivalent of H_2O_2 and Fe^{2+}. $NaNO_3$, $NaNO_2$, SIN-1 antibody were used as the source of NO_3^-, NO_2^- and ONO_2^-, respectively.

2.2. Synthesis of *DAN* and *DAN-T*

2.2.1. Synthesis of N-n-butyl-3,4-diamino-l,8-naphthalimide (*DAN*)

To a 50 mL round bottom flask equipped with magnetic stirrer, 3,4-diamino-1,8-naphthalic anhydride [19] (456 mg, 2.0 mmol) and dry 2-methoxyethanol 20 mL were added. The flask was placed in an oil bath heated to 50 °C and the solution of *n*-butylamine (439 mg, 6.0 mmol) and 2-methoxyethanol (5 mL) was added. Then the mixture was reflux for 8 h at 125 C. After the completion of the reaction, the reaction mixture was poured into 40 mL ice water and the red precipitate formed was filtered, washed with water and dried. The residue was purified by silica gel column (CH_2Cl_2:CH_3OH = 10:1) to give **DAN** 334 mg in 59% yield. Mp: >300 °C ^{1}H NMR (400 MHz, DMSO-d_6) δ 8.49 (d, J = 8.4 Hz, 1H), 8.20 (d, J = 13.6 Hz, 1H), 7.92 (s, 1H), 7.55 (t, J = 10.6 Hz, 1H), 6.50 (s, 2H), 5.19 (s, 2H), 4.00 (m, 2H), 1.57 (t, J = 11.2 Hz, 2H), 1.33 (m, 2H), 0.92 (d, J = 7.3 Hz, 3H). ^{13}C NMR (100 MHz, DMSO-d_6), δ 163.96, 163.18, 136.30, 130.43, 127.12, 123.65, 123.19, 121.65, 120.78, 119.55, 108.31, 38.85, 29.85, 19.82, 13.73. HRMS (EI): m/z 283.1322, $C_{16}H_{17}N_3O_2$ requires 283.1321.

2.2.2. Synthesis of 1H-1,2,3-triazole fused N-n-butyl-naphthalimide (*DAN-T*)

To a 25 mL round bottom flask equipped with magnetic stirrer, **DAN** (142 mg, 0.5 mmol) was dissolved in a mixture solvent of glacial acetyl acid (3 mL) and HCl (w = 36.5%, 1 mL) at 0 °C. Then the solution of $NaNO_2$ (69 mg, 1.0 mol) in H_2O (2 mL) was added at 0 °C. After 1 h, the ice bath was removed and the reaction mixture was stirred at room temperature for another 2 h. After completion of the reaction, the solvent was evaporated and the residue was purified by silica gel column chromatography (CH_2Cl_2:CH_3OH = 50:1) to obtain the product **DAN-T** 30 mg in 20% yield. Mp: 290.1 °C ^{1}H NMR (400 MHz, DMSO-d_6), δ 8.83 (m, 2H), 8.53 (d, J = 7.4 Hz, 1H), 8.04 (t, J = 7.8 Hz, 1H), 4.05 (m, 2H), 1.63 (m, 2H), 1.38 (m, 2H), 0.94 (t, J = 7.3 Hz, 3H). ^{13}C NMR (100 MHz, DMSO-d_6), δ 164.06, 163.48, 141.40, 137.03, 127.70, 137.92, 125.85, 124.49, 135.25, 127.38, 130.65, 117.81, 39.58, 29.85, 19.82, 13.73. HRMS (EI): m/z found 294.1118, $C_{16}H_{14}N_4O_2$ requires 294.1117.

3. Results and discussion

We first investigated fluorescent properties of **DAN** with the addition of NO in a mixture of ethanol and Tris–HCl buffer solution (50 mM, 1:1, v/v, pH 7.4). Kinetic profile of **DAN** (10 μM) with NOC13 solution (10 μM) displays that the fluorescent intensity of **DAN** could reach the maximum within 10 min partly as a result of gradual release of NO. Therefore, all the spectroscopic figures were obtained 15 min later after the addition of NOC13 solution to ensure the reaction reaching the equilibrium (Fig. S1, Supplementary Data).

3.1. The optical behavior of *DAN* with NO

To examine the fluorescent performances of **DAN** for the detection of NO, a fluorescent titration experiment was conducted. The free chemosensor **DAN** exhibits a quite weak fluorescence under physiological condition. With the addition of NOC13, the fluorescence intensity peaked at 454 nm increased proportionally (Fig. 1a) which was attributed to the interaction between the PET of 3-amino and the ICT of 4-amino in the fluorophore. The PET effect of the 3-amino group was inhibited leading to the increase in the emission intensity. Meanwhile, the ICT effect of the 4-amino group induced the blue shift of the emission wavelength compared with around 530-nm emission wavelength of 4-amino-1,8-naphthalimide [11]. When 1.6 equivalents of NOC13 were added to the solution of **DAN** (10 μM), the emission intensity reached the maximum (Fig. S2) that is ca. 160-fold enhancement colored in bright blue. This is due to the slow release of NO and the equilibrium of the reaction between NO and **DAN**. The ratio in the emission intensity (F/F_0) at 454 nm exhibits a good linear relationship with the concentration of NO between 0 and 16 μM (Fig. 1b). The ratio of F/F_0 is also in an NO concentration-dependent manner in lower concentrations of NO. The detection limit of **DAN** for sensing NO is determined to be ~19 nM (Fig. S3).

As displayed in Fig. 2, in the absence of NO, the free chemosensor **DAN** (10 μM) displays a strong absorption band around 476 nm and a weak band around 371 nm. With the addition of NOC13 solution, the absorption of **DAN** centered at 476 nm gradually decreased and the peak at 371 nm increased simultaneously with a distinct isosbestic point at 407 nm. When NOC13 solution (16 μM) was added to the solution of **DAN**, the absorption peak at 476 nm disappeared entirely and the peak at 371 nm reached the maximum value (Fig. S4) accompanied with a color change from yellow to colorless which indicates that **DAN** could be used as a colorimetric chemosensor to visualize NO by naked eyes under physiological condition.

3.2. The selectivity of *DAN* for NO

The selectivity of **DAN** toward various reactive oxygen species (ROS) and reactive nitrogen species (RNS) including NO, ClO^-, H_2O_2, $^1O_2$, •OH, NO_3^-, NO_2^-, ONO_2^-, was also assessed in the fluorescent and absorption spectra. As shown in Fig. 3a and b, none of these species induced appreciably fluorescence or absorption change except NO. This means **DAN** has a high selectivity for NO.

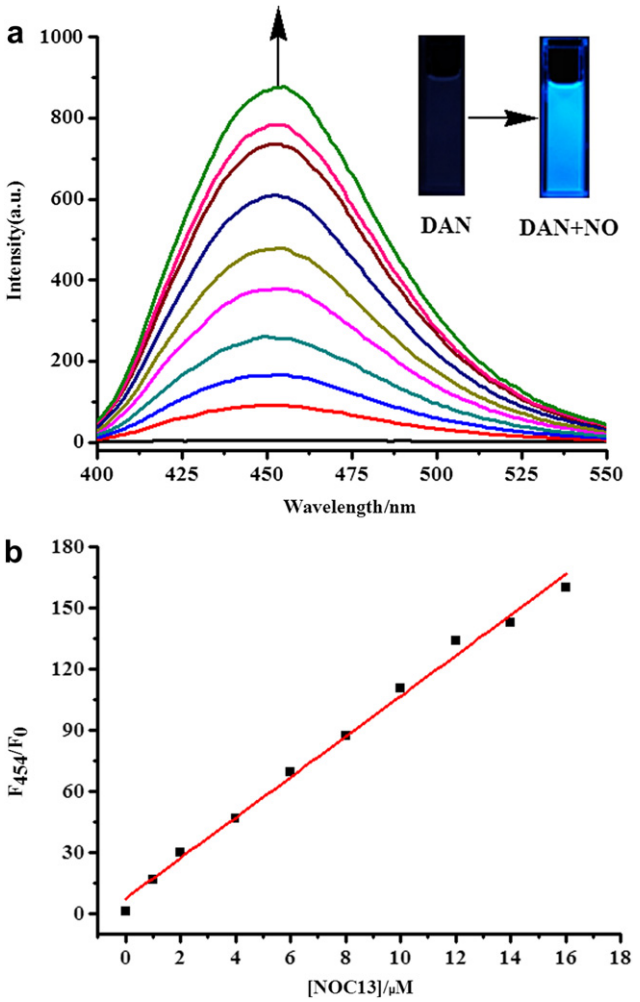

Fig. 1. (a) Fluorescence changes of **DAN** (10 μM) upon addition of NOC13 (0–16 μM). Inset shows the visible emission of **DAN** (10 μM) in the absence of NOC13 (left) and in the presence of 20 μM NOC13 (right). (b) Fluorescence intensity changes (F/F_0) at 454 nm of **DAN** (10 μM) upon addition of NOC13 solution (0–16 μM) in ethanol–Tris–HCl buffer (50 mM, pH 7.4) solution (1:1, v/v, rt). Excitation at 370 nm.

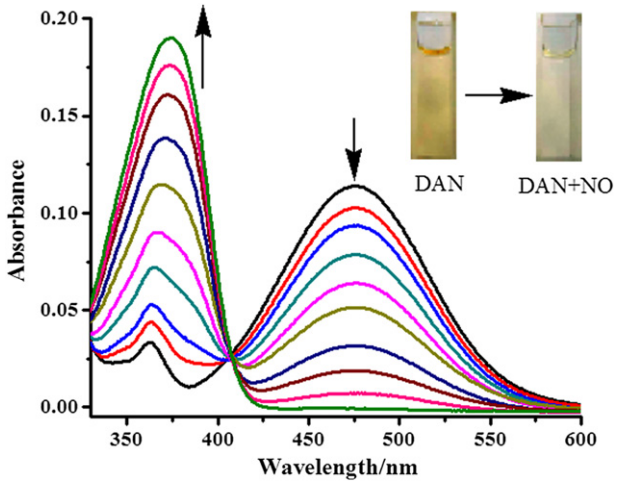

Fig. 2. Absorption changes of **DAN** (10 μM) upon addition of NOC13 (0–16 μM). Inset shows the color changes of **DAN** (10 μM) in the absence of NOC13 (left) and in the presence of 20 μM NOC13 (right) in ethanol–Tris–HCl buffer (50 mM, pH 7.4) solution (1:1, v/v, rt).

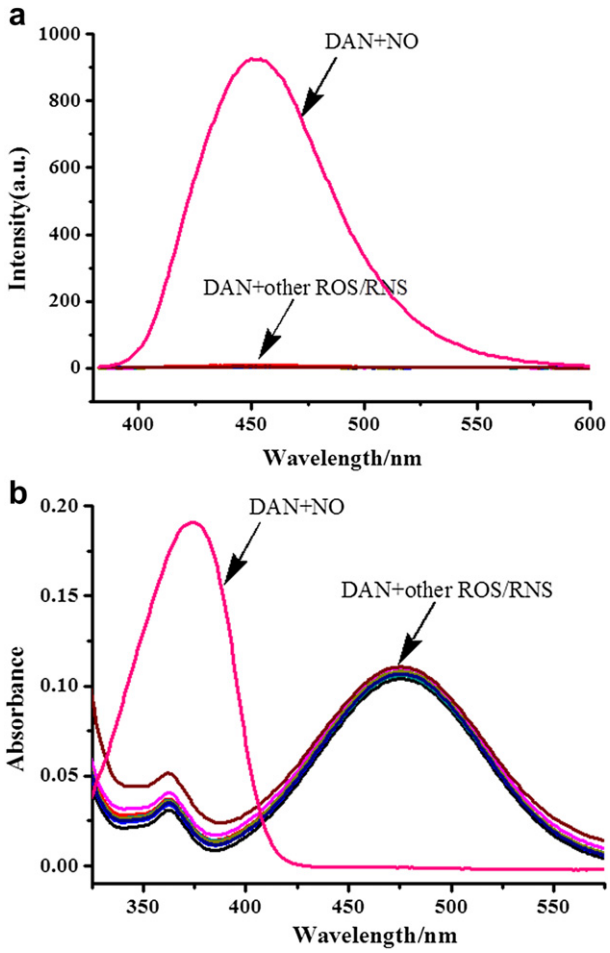

Fig. 3. (a) Absorption responses of **DAN** (10 μM) toward ClO^-, H_2O_2, $^1O_2$, •OH, NO_3^-, NO_2^-, ONO_2^- (50 μM) and NO (20 μM). (b) Fluorescence responses of **DAN** (10 μM) toward ClO^-, H_2O_2, $^1O_2$, •OH, NO_3^-, NO_2^-, ONO_2^- (50 μM) and NO (20 μM) in ethanol–Tris–HCl buffer (50 mM, pH 7.4) solution (1:1, v/v, rt). Excitation at 370 nm.

3.3. The effect of pH

Since most of fluorescent chemosensors with *o*-phenylenediamine as NO binding site are pH-dependent, we next evaluated the

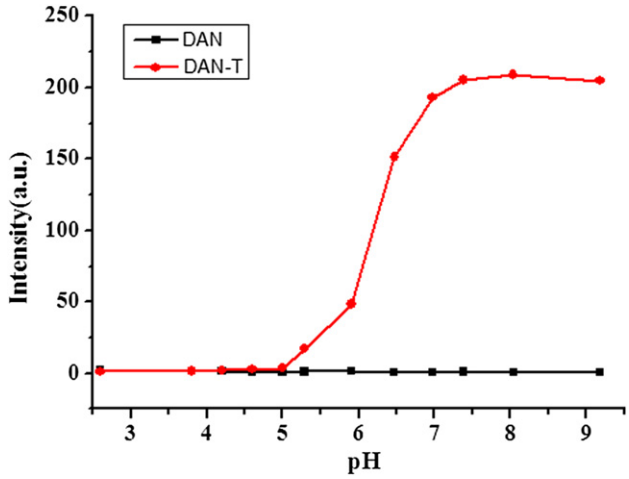

Fig. 4. Effects of pH on the fluorescence intensity of **DAN** (10 μM) and **DAN-T** (10 μM) at 454 nm in 50 mM buffer solution (pH 2.60–5.29 sodium acetate/acetic acid, pH 5.91–9.18 disodium hydrogen phosphate/potassium dihydrogen phosphate, rt). Excitation at 370 nm.

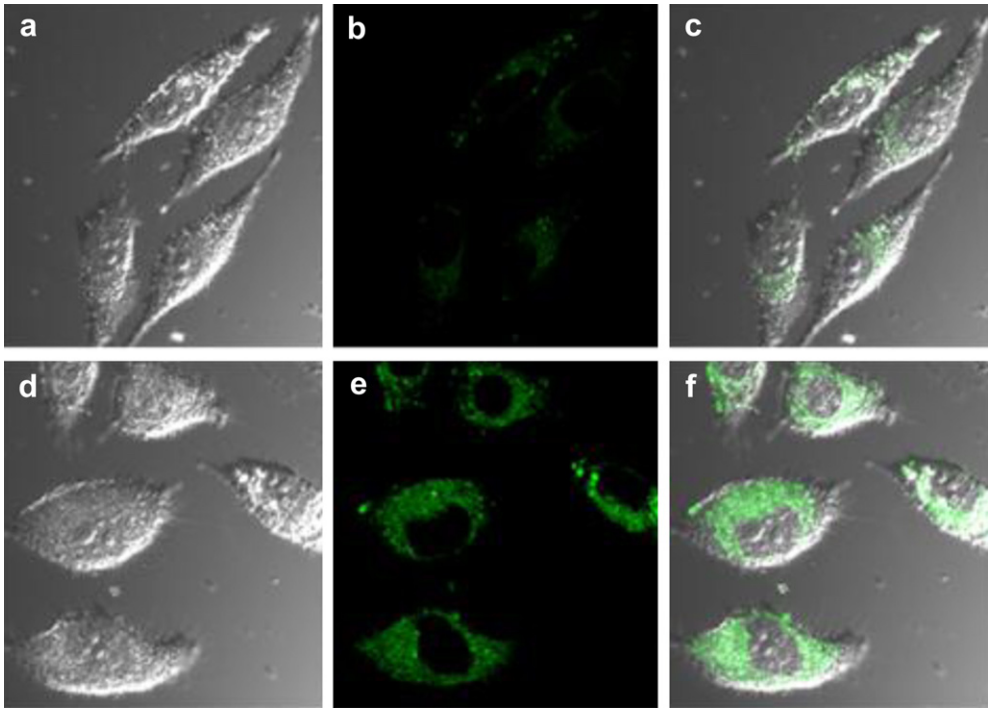

Fig. 5. Images of HT29 cells treated with the chemosensor **DAN**. (a) Bright field image of HT29 cells incubated with only **DAN** (10 μM) for 30 min; (b) Fluorescence image of (a) excited at 405 nm; (c) The overlay image of (a, b). (d) Bright field image of HT29 cells incubated with **DAN** (10 μM) and NOC13 solution (40 μM); (e) Fluorescence image of (d) excited at 405 nm; (f) The overlay image of (d, e).

effect of pH on the fluorescence of **DAN**. As shown in Fig. 4, **DAN** was nearly non-fluorescent from pH 2.6 to 9.3. We found that the emission intensity of the product **DAN-T** was very weak below pH 5, but strikingly increased above pH 5 and remained stable above pH 7 which demonstrated that **DAN** can work under physiological condition. This result was attributed to the formation of the triazole of **DAN-T** which inhibited the PET effect of the 3-amino group in 1,8-naphthalimide and that of the triazolate (the deprotonation form of the triazole) [20] which increased the electron-donating ability to induce the fluorescence enhancement.

3.4. Cell imaging of *DAN* with NO

We next applied the chemosensor **DAN** for fluorescence imaging of NO in HT29 cells (Human colon adenocarcinoma grade II cell line). After incubation with 10 μM **DAN** in culture medium for 30 min, HT29 cells showed a very weak fluorescence, as shown in Fig. 5. In contrast, another group of HT29 cells was incubated with 10 μM **DAN** for 30 min, then washed with phosphate buffered saline (PBS, 0.1 M, pH 7.4). After the addition of NOC13 solution (40 μM) for another 30 min, a strong emission signal was observed. The fluorescent signal from the cytoplasm of HT29 cells was verified by the overlap of the bright field and fluorescence imaging. These results demonstrate that the chemosensor **DAN** is cell-permeable and could be used to image intracellular NO.

4. Conclusion

We have successfully developed a “turn-on” fluorescent and colorimetric chemosensor for NO based on 1,8-naphthalimide. The chemosensor can be obtained via simple synthesis which shows high sensitivity and selectivity for NO and can be used to image NO at cellular level.

Acknowledgments

We thank financial supports from National Basic Research Program of China (2009CB724706) and Dalian Institute of Chemical Physics, Chinese Academy of Sciences.

Appendix A. Supplementary data

Supplementary data related to this article can be found at http://dx.doi.org/10.1016/j.dyepig.2012.08.024.

References

[1] Goldstein IM, Ostwald P, Roth S. Nitric oxide: a review of its role in retinal function and disease. Vision Res 1996;36:2979–94.
[2] Tare M, Parkington HC, Coleman HA, Neild TO, Dusting GJ. Hyperpolarization and relaxation of arterial smooth muscle caused by nitric oxide derived from the endothelium. Nature 1990;346:69–71.
[3] Bult H, Boeckxstaens GE, Pelckmans PA, Jordaens FH, Van Maercke YM, Herman AG. Nitric oxide as an inhibitory non-adrenergic non-cholinergic neurotransmitter. Nature 1990;345:346–7.
[4] Bogdan C. Nitric oxide and the immune response. Nat Immunol 2001;2:907–16.
[5] (a) Balligand JL, Kelly RA, Marsden PA, Smith TW, Michel T. Control of cardiac muscle cell function by an endogenous nitric oxide signaling system. Proc Natl Acad Sci U S A 1993;90:347–51;
(b) Pluth MD, Tomat E, Lippard SJ. Biochemistry of mobile zinc and nitric oxide revealed by fluorescent sensors. Annu Rev Biochem 2011;80:333–55;
(c) Thannickal VJ, Fanburg BL. Reactive oxygen species in cell signaling. Am J Physiol – Lung Cell Mol Physiol 2000;279:L1005–28;
(d) Ricciardolo FlM, Sterk PJ, Gaston B, Folkerts G. Reference values for exhaled nitric oxide (reveno) study. Physiol Rev 2004;84:731–65;
(e) Thomas CE, Darley-Usmar V. Forum on therapeutic applications of reactive oxygen and nitrogen species in human disease. Free Radic Biol Med 2000;28:1449–50.
[6] Zhang X. Real time and in vivo monitoring of nitric oxide by electrocehmical sensors–from dream to reality. Front Biosci 2004;9:3434–46.
[7] Bedioui F, Villeneuve N. Electrochemical nitric oxide sensors for biological samples–principle, selected examples and applications. Electroanalysis 2003;15:5–18.

[8] (a) Chen X, Zhou Y, Peng X, Yoon J. Fluorescent and colorimetric probes for detection of thiols. J Chem Soc Rev 2010;39:2120–35;
(b) Chen X, Tian X, Shin I, Yoon J. Fluorescent and luminescent probes for detection of reactive oxygen and nitrogen species. Chem Soc Rev 2011;40: 4783–804.

[9] (a) Kojima H, Hirotani M, Urano Y, Kikuchi K, Higuchi T, Nagano T. Fluorescent indicators for nitric oxide based on rhodamine chromophore. Tetrahedron Lett 2000;41:69–72;
(b) Suzuki N, Kojima H, Urano Y, Kikuchi K, Hirata Y, Nagano T. Orthogonality of calcium concentration and ability of 4,5-diaminofluorescein to detect NO. J Biol Chem 2002;277:47–9;
(c) Kojima H, Nakatsubo N, Kikuchi K, Kawahara S, Kirino Y, Nagoshi H, et al. Detection and imaging of nitric oxide with novel fluorescent indicators: diaminofluoresceins. Anal Chem 1998;70:2446–53;
(d) Sasaki E, Kojima H, Nishimatsu H, Urano Y, Kikuchi K, Hirata Y, et al. Highly sensitive near-infrared fluorescent probes for nitric oxide and their application to isolated organs. J Am Chem Soc 2005;127:3684–5;
(e) Nagano T. Bioimaging probes for reactive oxygen species and reactive nitrogen species. J Clin Biochem Nutr 2009;45:111–24;
(f) Nagano T. Development of fluorescent probes for bioimaging applications. Proc Jpn Acad Ser B Phys Biol Sci 2010;86:837–47.

[10] Lim MH, Lippard SJ. Metal-based turn-on fluorescent probes for sensing nitric oxide. Acc Chem Res 2007;40:41–51.

[11] Duke RM, Veale EB, Pfeffer FM, Kruger PE, Gunnlaugsson T. Colorimetric and fluorescent anion sensors: an overview of recent developments in the use of 1,8-naphthalimide-based chemosensors. Chem Soc Rev 2010;39:3936–53.

[12] Coskun A, Akkaya EU. Ion sensing coupled to resonance energy transfer: a highly selective and sensitive ratiometric fluorescent chemosensor for Ag(I) by a modular approach. J Am Chem Soc 2005;127:10464–5.

[13] (a) Xu Z, Xiao Y, Qian X, Cui J, Cui D. Ratiometric and selective fluorescent sensor for Cu^{II} based on internal charge transfer (ICT). Org Lett 2005;7:889–92;
(b) Xu Z, Qian X, Cui J. Colorimetric and ratiometric fluorescent chemosensor with a large red-shift in emission: Cu(II)-only sensing by deprotonation of secondary amines as receptor. Org Lett 2005;7:3029–32;
(c) Xu Z, Han SJ, Lee C, Yoon J, Spring DR. Development of off-on fluorescent probes for heavy and transition metal ions. Chem Commun 2010;46:1679–81;
(d) Xu Z, Yoon J, Spring DR. A selective and ratiometric Cu^{2+} fluorescent probe based on naphthalimide excimer-monomer switching. Chem Commun 2010; 46:2563–5;
(e) Xu Z, Pan J, Spring DR, Cui J, Yoon J. Ratiometric fluorescent and colorimetric sensors for Cu^{2+} based on 4,5-disubstituted-1,8-naphthalimide and sensing cyanide via Cu^{2+} displacement approach. Tetrahedron 2010;66:1678–83.

[14] Chen X, Wang J, Cui J, Xu Z, Peng X. A ratiometric and exclusively selective cu^{ii} fluorescent probe based on internal charge transfer (ICT). Tetrahedron 2011; 67:4869–73.

[15] (a) Xu Z, Qian X, Cui J, Zhang R. Exploiting the deprotonation mechanism for the design of ratiometric and colorimetric Zn^{2+} fluorescent chemosensor with a large red-shift in emission. Tetrahedron 2006;62:10117–22;
(b) Xu Z, Yoon J, Spring DR. Fluorescent chemosensors for Zn^{2+}. Chem Soc Rev 2010;39:1996–2006;
(c) Xu Z, Baek KH, Kim HN, Cui J, Qian X, Spring DR, et al. Zn^{2+}-triggered amide tautomerization produces a highly Zn^{2+}-selective, cell-permeable, and ratiometric fluorescent sensor. J Am Chem Soc 2009;132:601–10;
(d) Xu Z, Kim GH, Han SJ, Jou MJ, Lee C, Shin I, et al. An NBD-based colorimetric and fluorescent chemosensor for Zn^{2+} and its use for detection of intracellular zinc ions. Tetrahedron 2009;65:2307–12.

[16] Lu C, Xu Z, Cui J, Zhang R, Qian X. Ratiometric and highly selective fluorescent sensor for cadmium under physiological pH range: a new strategy to discriminate cadmium from zinc. J Org Chem 2007;72:3554–7.

[17] Xu Z, Zheng S, Yoon J, Spring DR. Discovery of a highly selective turn-on fluorescent probe for Ag^{+}. Analyst 2010;135:2554–9.

[18] Hrabie JA, Klose JR, Wink DA, Keefer LK. New nitric oxide-releasing zwitterions derived from polyamines. J Org Chem 1993;58:1472–6.

[19] Li F, Cui J, Guo L, Qian X, Ren W, Wang K, et al. Molecular design, chemical synthesis, and biological evaluation of '4-1' pentacyclic aryl/heteroaryl-imidazonaphthalimides. Bioorg Med Chem 2007;15:5114–21.

[20] Gabe Y, Urano Y, Kikuchi K, Kojima H, Nagano T. Highly sensitive fluorescence probes for nitric oxide based on boron dipyrromethene chromophore-rational design of potentially useful bioimaging fluorescence probe. J Am Chem Soc 2004;126:3357–67.